Remote Sensing of Environment 280 (2022) 113178

Contents lists available at ScienceDirect

Remote Sensing of Environment

journal homepage: www.elsevier.com/locate/rse

Assessing and modeling diurnal temperature buffering and evapotranspiration dynamics in forest restoration using ECOSTRESS thermal imaging

L. Jonas Hamberg[a,c,*], Joshua B. Fisher[b], Jonathan L.W. Ruppert[c,d], Jessica Tureček[e], Dean H. Rosen[a], Patrick M.A. James[a]

[a] Institute of Forestry and Conservation, John H. Daniels Faculty of Architecture, Landscape, and Design, University of Toronto, 33 Willcocks St., Toronto, ON, M5S 3E8, Canada
[b] Schmid College of Science and Technology, Chapman University, Orange, CA 92866, USA
[c] Toronto and Region Conservation Authority (TRCA), Vaughan, ON, Canada
[d] Ecology and Evolutionary Biology, University of Toronto, Toronto, ON, Canada
[e] School of Environment, Resources and Sustainability, Faculty of Environment, Waterloo, ON, Canada

ARTICLE INFO

Edited by Jing M. Chen

Keywords:
ECOSTRESS
Restoration ecology
24-h cycle
Diurnal
Forest
Applications
Evapotranspiration
Ecological restoration
Thermal imaging
Moderate resolution

ABSTRACT

Restoration of temperate forests alters the diurnal dynamics of land surface temperature (LST) and evapotranspiration (ET) through increases in biomass, diversity, and complexity. The ECOsystem Spaceborne Thermal Radiometer Experiment on Space Station (ECOSTRESS) is the first space-based thermal imaging instrument that allows for a study of diurnal LST and ET dynamics at a moderate spatial resolution (70 × 70 m).

We quantified, compared, and modeled the LST and ET dynamics of two groups of forest restoration sites (43 sites in total, between 2 and 75 ha) in Southern Ontario, Canada that were initially restored from mainly agriculture between 2007 and 2019. We included all useable LST ($n = 29$) and ET ($n = 9$) ECOSTRESS image products from a full growing season in 2020 (June 1st to September 30th). Forest restoration sites were compared by age and against agriculture (pre-restoration state), mature forest (post-restoration state), and suburban residential sites (competing land use).

The ability of forest restoration sites to buffer temperatures was highest in the afternoon, around 14:00 local time (EDT). As predicted, restoration sites were significantly cooler ($\bar{x}$ 4.4–7.4 °C) than residential and agricultural areas and significantly warmer ($\bar{x}$ 1.6–2.9 °C) compared to mature reference forest sites at both groups of sites. Relative diurnal (24-h) LST variability of forest and restoration sites was also significantly lower (0.9–2.9 °C) compared to agriculture and residential sites (3.3–5.2 °C). Daytime LST decreased significantly by 0.1 °C (3.1%), per year since restoration for one of the groups of sites relative to nearby mature reference forest sites as per a linear mixed effects regression model. It would take these sites ~30 years to reach the same buffering as mature forests. In characterizing ET dynamics of a subset of sites, we found that more recently restored sites had a statistically significant higher overall ET than older ones and that daytime relative instantaneous ET decreased with years since restoration. The variation explained by the ET model was however low.

Our study provides insights into how diurnal forest ecosystem energy conversion and storage dynamics changes over time after restoration. These diurnal thermal dynamics impact wildlife habitat as well as human wellbeing. The change in thermal buffering over time could be used to assess the pace and trajectory of restoration by managers. The thermal buffering provided by restored forest can also be quantified as an ecosystem service. As such, the study demonstrates the utility and also limitations of novel thermal remote sensing methods, using free and publicly available imagery from ECOSTRESS.

* Corresponding author at: Institute of Forestry and Conservation, John H. Daniels Faculty of Architecture, Landscape, and Design, University of Toronto, 33 Willcocks St., Toronto, ON, M5S 3E8, Canada
E-mail address: jonas.hamberg@utoronto.ca (L.J. Hamberg).

https://doi.org/10.1016/j.rse.2022.113178
Received 8 March 2021; Received in revised form 9 July 2022; Accepted 15 July 2022
Available online 23 July 2022
0034-4257/© 2022 Elsevier Inc. All rights reserved.

1. Introduction

Forest restoration is an integral part of achieving the United Nations Sustainable Development Goals (https://sdgs.un.org/goals/goal15). There are a growing number of large scale restoration, reforestation, and afforestation projects with ambitions of planting billions of trees in the coming decade (e.g., Broadhurst et al., 2016; Holl and Brancalion, 2020 suppl. Table 1). However, forest restoration projects often fail due to issues such as invasive species, disease, or use of planting stock or seed inappropriate for the site (Holl and Brancalion, 2020; Ruiz-Jaen and Aide, 2005; Stanturf et al., 2014). Restoration scientists point to an urgent need for more efficient and scalable monitoring to understand ecological processes underlying restoration success or failure, in order to improve forest restoration outcomes (DeLuca et al., 2010; Holl and Brancalion, 2020; Reif and Theel, 2017).

Remote sensing can be used to assess ecosystem processes and monitor the success of restoration projects (Reif and Theel, 2017). Remote thermal imaging holds particular potential for monitoring land surface temperature (LST) and evapotranspiration (ET), both of which can used to assess physiological plant functions, drought stress and changes in biomass, canopy cover, plant diversity, and complexity in forest ecosystems (Ehbrecht et al., 2019; Fisher et al., 2017; Hamberg et al., 2020; Lin et al., 2017). A thorough understanding of the connection between these ecosystem functions and structure can help managers plan, adapt, and monitor their restoration projects more effectively. However, the change in LST and ET after restoration, as measured by thermal imaging, remains largely unexplored.

The LST of a forest is regulated by the reflection, storage, and conversion of solar energy. The relative rate at which the ecosystem reflects, stores, and converts the incoming energy depends on the albedo, emissivity, physical heat capacity, and ET rates of vegetation and soil (Fisher et al., 2017; Meier et al., 2019; Michaletz et al., 2015). ET rates in turn depend on solar energy input, photosynthetic biomass available, soil-water availability, wind, and humidity (Fisher et al., 2017). Many of the factors which affect LST and ET are, in turn, influenced by spatial and temporal variation in forest ecosystem structure and function.

Daytime LST tends to decrease as forest biomass and age increases (Lin et al., 2017; Naranjo et al., 2012). Forest plant diversity also affects LST and ET (Baldocchi, 2005; Hamberg et al., 2020; Norris et al., 2012). Plant diversity increases the variety of vertical and horizonal stand structure, above-and below-ground plant structures (e.g., rooting depths), ecosystem functions (e.g., photosynthetic pathways), and variation in phenology (e.g., leaf-out timing). This increase in variation improves the overall uptake of water and interception and conversion of solar energy, thereby moderating LST and ET during different parts of the day and year, and during different weather and ground water conditions (Baldocchi, 2005; Hamberg et al., 2020; Norris et al., 2012). Increased forest diversity and complexity can also increase physical and chemical energy storage capacity as it increases with increased living and dead biomass distributed vertically, horizontally, and through time (Ehbrecht et al., 2019; Meier et al., 2019; Norris et al., 2012). This increased energy storage capacity further serves to buffer daily LST variation (Ehbrecht et al., 2019; Meier et al., 2019).

Thermal buffering refers to the ability of vegetated sites to moderate and reduce diurnal (24-h) temperature variation away from extremes (Lin et al., 2020). Thermal buffering reduces LST at peak daily insolation (solar noon) and delays the release of heat energy later into the day, potentially increasing night-time temperatures (Chen et al., 1999; Hamberg et al., 2020; Lin et al., 2020). In general, temperate forests buffer temperatures better than non-forest ecosystems in the same climate, and buffering capacity increases with forest biomass (Chen et al., 1999; Holmes et al., 2015; Meier et al., 2019). The thermal buffering effects of forest vegetation are important for creating suitable habitat conditions for many organisms (Tuff et al., 2016). Ecological restoration projects often aim to return native flora and fauna by creating suitable habitat (Stanturf et al., 2014; Suganuma and Durigan, 2015; Tuff et al., 2016). Improving a forest's thermal buffering capacity is therefore a potentially useful target for restoration, but one that is so far understudied, especially using thermal imaging.

In addition to LST, ET is an integral ecosystem process that may also be used to monitor the progress and efficacy of restoration. Diurnal ET dynamics depend on species composition, climate, topography, and previous land use (Filoso et al., 2017; Naranjo et al., 2012). ET in temperate forests increases with time of day past solar noon, although extreme summer temperatures can cause an afternoon depression where plants reduce transpiration to avoid excess water loss (Bonan, 2008; Xiao et al., 2021). The effects of different types of forest restoration and afforestation on ET dynamics are complex. The increased water demand of low-diversity afforestation and commercial plantations species unsuitable for the site conditions can decrease water yield, cause local drought, and lead to their own failure, especially in already water-limited areas (Filoso et al., 2017; Holl and Brancalion, 2020) Diverse and locally adapted temperate forest restoration has, on the other hand, been shown to improve ET seasonal and diurnal regulation and reduce the risk of drought (Baldocchi, 2005), particularly over long time scales (> 20 years) (Filoso et al., 2017; van Dijk and Keenan, 2007). More efficient and cost-effective methods for ET monitoring can help managers assess the progress of their restoration sites towards an ET dynamic similar to that of a mature forest and adapt management and tree species planted to site and climate conditions.

We currently know relatively little about how diurnal LST and ET changes over time in response to active forest restoration, as opposed to passive recovery and succession. Active restoration, through planting, seeding, or other interventions, is meant to guide and accelerate forest succession (Stanturf et al., 2014). If active restoration accelerates forest recovery and succession – increasing biomass, diversity, and ecosystem complexity – then it should also accelerate change in diurnal LST buffering and ET dynamics. However, depending on site size, distance to seed-sources, former land-use, and soil conditions, active restoration methods are not always faster or more effective than passive recovery

Table 1
Detailed summary and comparison of the NCC and TRCA group of sites and image products used.

	NCC	TRCA
Number of restoration sites	35	8
Number of forest sites	35	8
Number of agricultural sites	12	8
Number of residential sites	0	4
Median size of restoration areas	10.0 ha	3.8 ha
Median size of restoration areas with 50 m buffer excluded	3.68 ha	0.7 ha
Pre-restoration conditions	Agriculture, old fields, and marginal land	Agriculture, old fields, and marginal land
Type of restoration	High diversity seeding of herbaceous, shrub and tree species (~80–100 species)	Planting of bareroot, seedling and sapling shrubs and trees (3–14 species)
Initial year of restoration represented (number of sites that year)	2007 (4), 2008 (3), 2009 (1), 2010 (1), 2011 (4), 2012 (7), 2013 (7), 2014 (1), 2018 (4), 2019 (3)	2007 (2), 2008 (1), 2009 (2), 2010 (1), 2013 (1), 2018 (1)
Number of image products used	19 LST, 9 ET	15 LST
Date range for imagery in 2020	June 6th – September 23rd	June 6th – September 25th
Maximum diurnal time data gap (LST)	04:19–09:44 (5 h, 25 min)	01:14–08:27 (7 h, 13 min)
View angle of imagery (mean / max)	16.7° / 28.1°	12.3° / 26.2°

and succession (Londe et al., 2020; Meli et al., 2017). A common question among restoration managers is when a project can be projected to be 'done', in terms of when the project functions and provides services at a rate similar to that of a mature forest (Ruiz-Jaen and Aide, 2005; Stanturf et al., 2014). Long-term monitoring of relative change in the LST buffering and ET of restoration projects could allow managers and scientist to tell which methods actually accelerate succession towards that of a reference/goal state, and at what rate.

The unique characteristics of ECOSTRESS provide opportunities to measure diurnal LST and ET change in sites smaller than was previously possible to study with satellites (< 100 ha). Diurnal temperature and ET have been previously measured using ground-based tools such as eddy covariance flux-towers (Fisher et al., 2011). Satellite-based thermal imagers also provide opportunities to measure LST and ET over large spatial extents. However, satellite thermal imagers with a high or varied enough temporal resolution to measure diurnal change have been limited by their coarse spatial resolution. Studies of diurnal dynamics have used thermal imagers such as Moderate Resolution Imaging Spectroradiometer (MODIS) and Himawari which have high temporal resolution ($\geq$ 1 day), but coarse spatial resolution ($\geq 1 \times 1$ km) (e.g., Oyoshi, 2014; Qiao et al., 2013), thereby having to focus on regional or larger dynamics. In comparison, the ECOSTRESS instrument's products have a 70×70 m gridded spatial resolution and a 1–5 day revisit time. Actual spatial resolution of ECOSTRESS is affected by the zenith view angle of the imagery acquired due to the 'push whisk-broom' image acquisition movement of the focal plane of the instrument. Actual resolution has its finest resolution of 69×38 m at nadir (0°) but resolution decreases with view angle, up to the maximum angle of ~26° (Anderson et al., 2021). The ECOSTRESS instrument on the International Space Station (ISS) consists of a thermal infrared radiometer with five bands (three active) allowing for accurate emissivity corrections (Hook et al., 2019). Most importantly, the precessing orbit of ISS and ECOSTRESS results in revisits at a different local time each orbit, allowing for modeling of diurnal dynamics. The higher spatial resolution of ECOSTRESS is particularly useful as forest restoration sites are typically smaller than 1 km^2 (Cramer et al., 2008; Londe et al., 2020; Stanturf et al., 2014), and are often narrower than 1 km, such as in the case of restoration of riparian zones, roads, or power-corridors (e.g., Suganuma and Durigan, 2015). ECOSTRESS LST and instantaneous ET measurements have shown a high degree of agreement with ground-based eddy covariance measurements and ground-based temperature targets (Fisher et al., 2020; Hook et al., 2019). A preliminary study using ECOSTRESS data from only late summer 2018 found that forest restoration decreased diurnal variability through decreasing maximum daytime LST and increasing night-time minimum LST (Hamberg et al., 2020).

In this study, we use ECOSTRESS data to compare and quantify the pace and trajectory of forest restoration in terms of relative mean daytime LST and ET and relative diurnal LST and ET variability and dynamics. ET and LST is measured relative to nearby mature forests to normalize ECOSTRESS data captured on different days, we refer to these measures as relative land surface temperature (RLST) and relative evapotranspiration, instantaneous (RETi). We specifically address the following three questions: 1) What is the relative difference in diurnal LST and ET dynamics between a starting, or 'pre-restoration', state of agriculture, ongoing forest restoration, mature forest sites similar to the target state of restoration and, the competing land use of residential suburban sites? 2) How does relative LST and ET change with the age of restoration sites? And 3) how long does it take for a restoration area to reach the same surface temperature and ET as the mature forest sites? Through these measurements and multiple comparisons, we present a gradient of LST and ET from residential, to agricultural, to different stages of restoration, to intact forest. Understanding LST and ET dynamics along this gradient is important to improve forest management and restoration as these dynamics reflect the speed, efficacy, and trajectories of forest recovery and restoration efforts.

We hypothesize that increases in biomass and plant function and structure will decrease summer daytime RLST and increase diurnal thermal buffering capacity. Specifically, we predict that forest restoration sites will exhibit lower summer daytime RLST at their daily peak, and lower diurnal RLST variation, than agricultural sites (pre-restoration state), but higher than mature forest sites (post-restoration-state). We also predict that the suburban residential sites, with its roads, buildings, and low-biomass lawns to be hottest and have the least buffering. We hypothesize that RETi will be affected by biomass, ecosystem function, irrigation (croplands and lawns), and overall soil-water availability. However, due to the complexity of water availability and use, we do not predict whether forest restoration would have higher or lower RETi than other land uses. We do however predict that REti, as well as RLST, of restoration sites will converge with that of mature forest sites as the restoration sites increase in biomass, diversity, complexity, and canopy coverage towards a mature state (30–50 years). Answering these questions and testing our predictions will increase our theoretical understanding of how diurnal LST and ET dynamics change with forest restoration, which in turn improves our ability to effectively monitor and assess the pace and trajectory of forest restoration projects using ECOSTRESS and similar moderate resolution thermal imagers.

2. Methods

2.1. Study sites

Two groups of restoration sites in southern Ontario, Canada were selected for this study (Fig. 1). These are large but fragmented groups of temperate forest restoration projects of varied ages which were mainly restored from former agriculture fields. The two groups of sites differed in restoration methods, species mix, soil conditions, and geographic locations.

The first group of sites, located in Norfolk County, Ontario is part of a restoration and conservation project by Nature Conservation of Canada (NCC) (Fig. 1A). The NCC project includes 51 separate properties where restoration and/or conservation has, or will be, undertaken on one or more separate fields (Nature Conservancy of Canada, 2006). Restoration at NCC sites was conducted using a high diversity seed-mix (~80–100 species) to transform formerly agricultural land into oak-savannah and oak woodland (Nature Conservancy of Canada, 2006). Restoration was conducted incrementally with the 'oldest' site initially restored in 2006 and the most recent site in 2019. In total, the project has initiated restoration of 742 ha as of 2020. The restoration and conservation sites are sub-divided into five management blocks by the NCC (black circles in Fig. 1A). The landscape around the restoration sites consisted mainly of mixed deciduous forest and agriculture, including corn, tobacco, soy, and ginseng (site visits, Norfolk County, ON, August 2020).

The second group of restoration sites were implemented by the Toronto and Region Conservation Authority (TRCA) within Caledon, Peel Region, between 2007 and 2018 (Fig. 1B). The area includes approximately 60 different restoration projects and sites over a total of 170 ha. Forest restoration at TRCA sites was conducted mainly on former agricultural and marginal land through mechanical or hand planting of seedlings and saplings of shrubs and tree species, including cedar (*Thuja* sp.), dogwood (*Cornus* sp.), maple (*Acer* sp.), willow (*Salix* sp.) and pine (*Pinus* sp.) species. The landscape around sites consists of agricultural fields (including corn, soy, and wheat (site visits, Peel Region, ON, August 2020)), forests, tree plantations, and low-density suburban residential areas.

2.2. Site selection

Restoration sites were included in the study if they were being restored towards a forested state on mainly former agricultural land. The restoration sites were then compared to active agriculture sites similar to the 'pre-restoration' starting state of restoration sites, mixed deciduous forest sites similar to the 'post-restoration' target state of the restoration

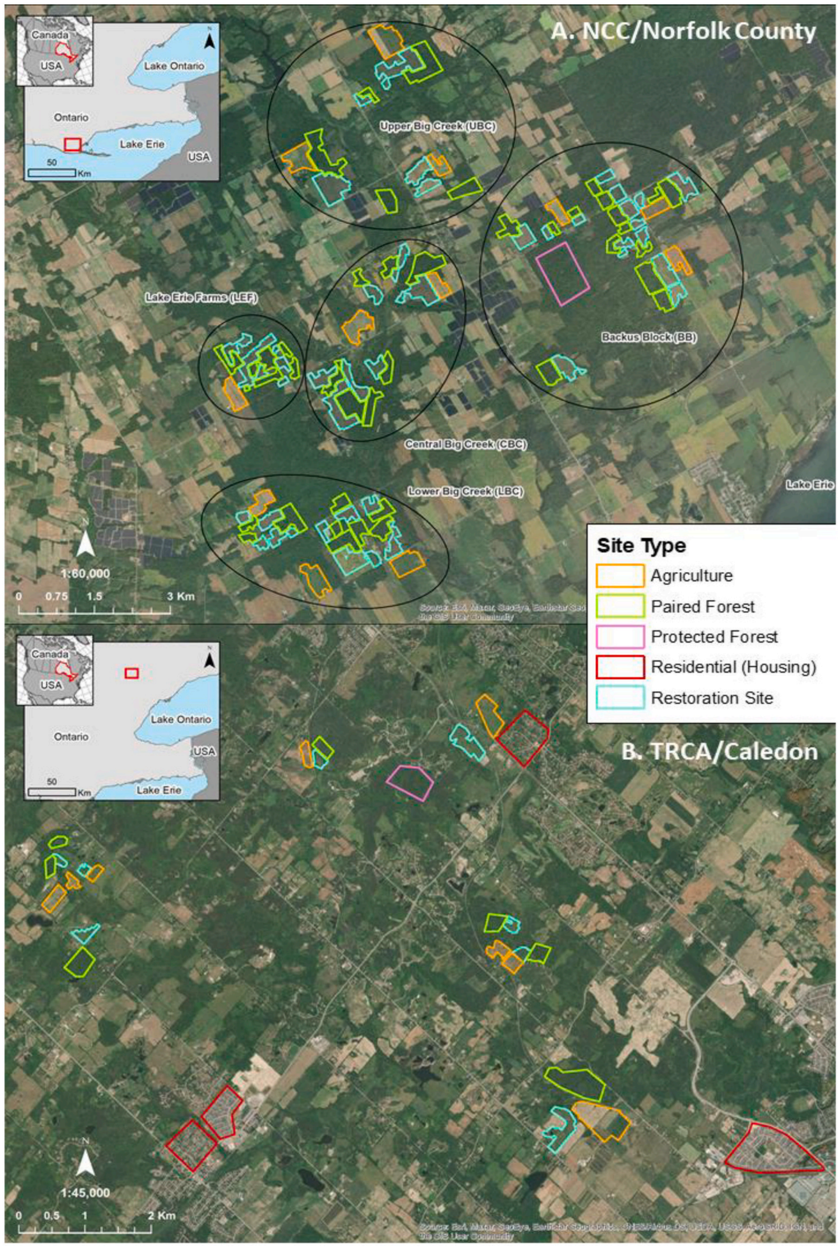

Fig. 1. (A) Map of the NCC group of sites in Norfolk County and (B) the TRCA group of sites in the Town of Caledon. Black ovals show five management blocks used by NCC. In the top left insert maps, the red areas show the location of Ontario and the area of interest within Ontario respectively. Base imagery from Esri et al. (2021). (For interpretation of the references to colour in this figure legend, the reader is referred to the web version of this article.)

projects. We also include sub-urban residential areas due to it being a competing land-use of former farmland.

Restoration sites were included if they were larger than 2 ha and wider than 100 m. Two ha equal approximately four 70 × 70 m pixels in ECOSTRESS imagery. Each site's vector polygon was decreased by a 50 m internal buffer to limit the thermal effects of the surrounding landscape on the area of interest (Tuff et al., 2016). Sites which had prescribed burns ($n = 3$) were excluded from the study.

In total, 35 restoration sites were included for the NCC group, with a mean site size of 12.6 ha, ranging between 3.9 and 31.4 ha (Fig. 1A, teal polygons). These 35 sites represented initial restoration in 10 different years within the span of 2007–2019 (Table 1). Eight restoration sites were included for the TRCA group, with a mean site size of 6.1 ha and a range between 2.1 and 15.3 ha (Fig. 1B, teal polygons). TRCA sites represented six different years of initial restoration between 2007 and 2018.

A paired area of mature forest was chosen as a reference ecosystem for each restoration site in both the NCC and TRCA groups (Fig. 1, green polygons). The criteria for paired mature forest area selection were full canopy cover of mixed deciduous forest; approximately similar in size and shape to the restoration areas; as close as possible to the restoration site. The maximal distance between paired restoration and forest sites was 700 m, with 36 out of 43 pairs directly adjacent to each other. Forest maturity and intactness was selected based on visual inspection of aerial imagery from 1954 and visual Landsat imagery from 1984 to 2020 (Hunting Survey Corporation Limited, 1954; U.S. Geological Survey, 2016).

Along with the smaller paired mature forest areas, two larger mature protected forests were also selected as references to allow for intra-seasonal comparisons between all land-covers with a stable and relatively predictable area (see section 2.4). The largest intact protected non-plantation forest in each area was selected – Backus Woods (BW)

Nature Preserve for the NCC group of sites, and Albion Hills (AH) Conservation Park for the TRCA group of sites (Fig. 1, pink polygons). Both these sites have been protected from logging or development since 1955 (Curran, 2018; Strader, 2017).

Active non-shaded agriculture was identified using summer 2020 Landsat 8 visual and Normalized Difference Vegetation Index (NDVI) imagery through the LandLook Viewer (https://landlook.usgs.gov/). Agricultural sites were selected based on closeness to restoration sites and approximately similar size and shape to restoration sites. Twelve agricultural sites were included for The NCC area (three for each restoration block) and eight for the TRCA area (Fig. 1, orange polygons).

Site selection of residential sites was based on proximity to restoration sites and similarity in size. Four areas within the TRCA group containing suburban residences were included in this study (Fig. 1B, red polygons). Residential sites were not included for the NCC area as it is more rural and does not include large enough residential areas.

2.3. Imagery selection and processing

All ECOSTRESS products are free and publicly available to download through the AppEEARS tool (https://lpdaac.usgs.gov/tools/appeears/). LST data products from ECOSTRESS are corrected for emissivity and atmospheric conditions (Hulley and Freepartner, 2019). The Priestley-Taylor Jet Propulsion Laboratory (PT-JPL) evapotranspiration product used in this study inputs results from the ECOSTRESS LST product, along with data from MODIS, Landsat and/or ground-level weather stations, into an algorithm based on the Priestly-Taylor equation for ET (Fisher et al., 2020). This study used the instantaneous ET product, which is measured in W/m^2 as it represents the energy transformed through latent heat flux as water is vaporized.

All ECOSTRESS LST imagery for the groups of sites in the growing season (June 1st to September 30th) of 2020, as well as quality control (QC) and cloud layers, were examined for their useability. Imagery was removed if extensive quality issues were identified or if clouds covered >20% of the study areas. Nineteen usable LST images were included of the NCC group area, and 15 of the TRCA group area (Fig. 2).

For included imagery, pixels identified as cloud-covered or low quality (QC layer bit-value) were removed (Fisher et al., 2020; Hulley and Freepartner, 2019). LST and ET mean values were extracted for each field vector using the Zonal Statistics tool in QGIS. Site values were only included in the analysis if pixel removal due to cloud cover or quality issues was <25% of total pixels for that site. ECOSTRESS zenith view angle affects actual pixel size. For reference we calculated view angle as the mean for each group of sites for each imagery and report mean and max view angle of all imagery for each group of sites in Table 1. We did not set a maximum for view angle or exclude imagery because of it.

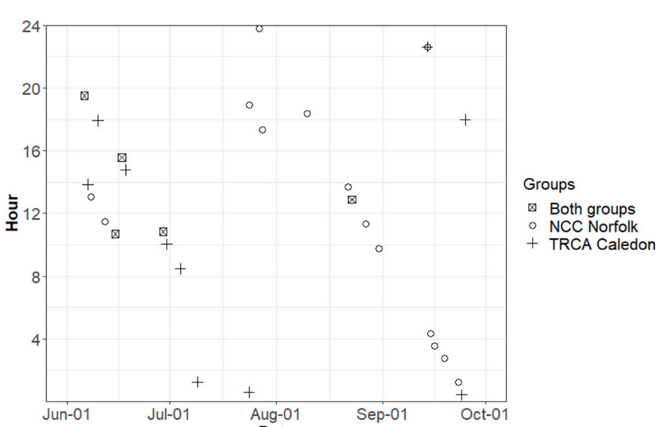

Fig. 2. Date and time during the day of capture of each ECOSTRESS thermal image used in this study.

Graphs of view angle by date and group of sites for each image are available in Appendix A.

From the PT-JPL ET product, we used the instantaneous ET (Eti) product in this study. Due to the requirement of cloud-free data from MODIS to execute the ET calculation, and as ET is only calculated during daytime, there are fewer ET products than LST ones. Usable ET products were limited to nine for the NCC group area and three for the TRCA group area. We considered the three data points of TRCA sites to be insufficient for diurnal comparisons and modeling and therefore only included the NCC group of sites for ET tests.

ECOSTRESS aims for a 50 m geolocation accuracy to ground (Smyth and LePrince, 2018). However, due to uncertainty of ISS positioning, and at times with less pronounced thermal difference (night especially), 5 images showed errors up to 3 km. To fix this error, LST and ET images were georeferenced to a base-map manually in QGIS (QGIS Development Team, V 3.16), where necessary to achieve <50 m accuracy. Small lakes, road intersections, and other thermally distinct areas were used as georeferencing points.

2.4. Statistical analysis

The precessing orbit of ECOSTRESS allows for observations at different times of the 24-h day, multiple times during a season. However, it generally does not provide multiple images from the same day. Therefore, to study differences in relative diurnal LST and ET dynamics we first compressed all data acquired from ECOSTRESS on different dates into a single 24-h cycle. Then, to control for daily insolation and weather variability, we calculated the relative land surface temperature (RLST) and relative instantaneous evapotranspiration (RETi) for all sites relative to that of mature reference forest areas. When comparing multiple site types, we calculated RLST and RETi as the mean value of the site of interest minus the mean value of a large mature and protected reference forest area (Fig. 1, pink polygons). For example, comparing LST between site types, the formula would be: $\overline{LST}_{\text{site of interest}} - \overline{LST}_{\text{large protected mature forest site}} = \text{RLST}$. When comparing only forest restoration sites to each other, RLST and RETi were calculated relative to nearby paired mature forest areas (Fig. 1, green polygons), in the same image. Paired mature forest sites provide closer comparisons to each restoration site, than one large, protected site but pairing was not possible when comparing all site types. For all results involving RLST and RETi, the large mature protected forest area or paired mature forest area used for comparison has its value subtracted from itself, creating the zero-line in graphs and plots. Note that our use of RETi is different from when actual ET is compared to potential ET, which has also been referred to as relative or reference ET.

Similar methods have been used for comparing relative temperature change over time in thermal remote sensing (e.g., Cai et al., 2019; Elsen et al., 2020). However, unlike other studies that have used the mean of the full study area (Cai et al., 2019) or a central pixel within a moving window (Elsen et al., 2020) as the relative comparison, our approach uses nearby mature forest areas which are expected to have a relatively similar response to variation in insolation and weather, and thereby LST, throughout the area of interest (Hamberg et al., 2020; Lin et al., 2020; Michaletz et al., 2015). Calculating the temperature relative to a nearby mature forest area should also be physically and eco-physiologically closer to our sites of interest than using the full study area or a central pixel. Adjusting for intra-seasonal change in photosynthetic activity, biomass accumulation, and weather patterns for diurnal modeling is a challenge that has been discussed in the context of other satellite instruments. (Cai et al., 2019; e.g., Giglio, 2007). Currently, there is no ideal method or instrument that can remove all variability (Cai et al., 2019; e.g., Giglio, 2007). However, ECOSTRESS provides more observations at different diurnal times during the growing season than any other moderate resolution thermal imager so far.

High wind speed and/or humidity could affect RLST and RETi in ways unconnected to ecosystem function and energy conversion and storage (Bonan, 2008; Michaletz et al., 2015; Song et al., 2016). Based on literature, we removed imagery if wind speed exceeded 25 km/h or relative humidity exceeded 80% (Bonan, 2008; Michaletz et al., 2015; Song et al., 2016). Hourly measurements were taken from the nearest ground-level weather station available – 29 and 69 km from furthest site for NCC and TRCA respectively (Environment Canada, 2021). Wind-speed, humidity, air-temperature (noon and at hour of image), and 4-day precipitation graphs are available in Appendix A. No imagery had to be removed due to high wind speeds or humidity at the time of capture.

To better understand how forest restoration affects LST and ET we built a series of statistical models. In total nine models were developed, three each of RLST for the NCC and TRCA sites, and three of RETi for the NCC sites (Table 2). These models and tests applied to them are described in the following two sub-sections. For all following sub-sections, an alpha of 0.05 was applied to all statistical models for determining significance. All statistical analysis, diagnostics plots, and assumption tests performed in R (v. 4.0.3, R Project, 2020) are available in Appendix B. References to all R packages used are included in Appendix B. ANOVA and Welch's test on peak LST and ET were performed in XLSTAT (v. 2021.1.1, Addinsoft, 2021) and tests on their assumptions are available in Appendix C. All data are available in Hamberg (2022).

2.4.1. Analysis of difference in RLST

2.4.1.1. Comparing the RLST diurnal pattern of restoration with other site types. The difference in RLST between land cover site types (i.e., agriculture, forest restoration, paired mature forests and suburban residential (TRCA only)) was visualized using a spline regression fit to the diurnal data. Spline regression was selected over alternative regression methods (e.g., linear polynomial or sinusoidal regression) as it allows for a skewed daytime distribution and a flatter night-time curve. Spline regression is commonly used for interpolating diurnal peaks and visualizing time-series data (e.g., Aires et al., 2004; Cai et al., 2017; Chen et al., 2006; Gianinetto and Villa, 2007). We set spline knots to 4, 8, 12, 16 and 20 h, and used cubic splines. The knot at 20 h was omitted for the TRCA sites due to lack of images acquired near or at this time.

We next tested and quantified the differences in RLST among site types during the diurnal 'period of peak difference' using two-way ANOVA or Welch's corrected ANOVA. Diurnal 'period of peak difference' in RLST was defined as the two hours on either side of the time of maximal difference between restoration sites and the reference protected forest sites occurred as per the spline regression. For example, if the peak difference was identified at 14:00 local time, the period was from 12:00 to 16:00. The reason for choosing a 4-h period, rather than the exact peak, was to decrease the effect of any single thermal image measurement while still focusing on the time of day where RLST differences were greatest between site types. Beyond determining the peak of RLST for different site types (and thereby the imagery included in the 'period of peak difference'), the spline regression lines were not used for any statistical testing and only included for visualization. For the TRCA group of sites, we used a 2-way ANOVA with interaction to model how mean RLST varied as a function of the categorical variables of site type and image ID. Image ID was included to test the effect of including multiple images taken at different diurnal times. For the NCC sites, we used Welch's corrected ANOVA instead of classic ANOVA, as the assumption of equal variance of residuals required for ANOVA was not fulfilled. For all ANOVA in this study, the assumption of normality was tested using the Shapiro-Wilk test and that of equal variance using Levene's test. Where ANOVA results were significant, Tukey's HSD was used as the *post-hoc* test. The Games-Howell test was applied as the *post-hoc* pairwise comparison where Welch's test results were significant.

2.4.1.2. 24-h variation in RLST. We examined how diurnal (24-h) variation in RLST varied among sites. We were specifically interested in testing if restored sites exhibited increased thermal buffering (i.e., decreased diurnal temperature variation). Variation was measured as the standard deviation of the mean of RLST for each site over all included imagery. We used standard deviation in RLST as the response variable in a one-way ANOVA with site type as the categorical predictor. Standard deviation, as opposed to variance, of RLST is useful in this case as it represents the fields' respective diurnal LST variations from that of their associated protected forests' LST, while retaining the original unit of measurement. Significant differences were further tested and quantified using the Tukey-adjusted estimated marginal means (emmeans) *post-hoc* test, as it is adjusted for unbalanced paired models.

2.4.1.3. Modeling change in diurnal RLST with time since restoration. To investigate the potential difference in RLST with years since restoration, we first visualize diurnal RLST by graphing it against sites grouped by years since restoration. For visualization, restoration sites were grouped into three categories based on "years since restoration began": 1–5, 6–9, and 10–14 years. A cubic spline regression was applied to the grouped data. We set spline knots to 4, 12 and 16 h for NCC sites and 12 and 16 h for TRCA sites.

To test if years since restoration (fixed independent factor) had a significant effect on daily RLST (dependent factor), we used a linear mixed effects regression model. The model also included restoration site size and time from peak difference as fixed effect independent factors and site as a random factor, as there were multiple image measurements associated with each site. As we used sites of different age, within the same growing season, this is a space-for-time substitution model where years since restoration was treated as a discrete variable. We only include daytime measurements ($\pm$ 6 h from peak RLST difference, as established in section 2.4.1) in this model as we do not expect nighttime

Table 2
Summary of statistical models developed. Each model of RLST was developed separately for TRCA and NCC sites. Additional variables includes both fixed and random factors.

Measure and groups	Dependent variable	Reference site used for relative measurements:	Main independent variable	Additional Independent variables	Test	Imagery included
RLST - NCC and TRCA	Mean RLST	Large Protected Mature Forest	Site type: Agriculture, Restoration, Paired Forests, Residential*	Image ID	Two-way ANOVA /Welch's	Within $\pm$2 h of peak difference
	SD of 24-h mean RLST	Large Protected Mature Forest	Site type (as above)		One-way ANOVA	All
	Mean RLST	Smaller Paired Mature Forest	Years since restoration (discrete variable)	Size, time from peak, site name	Linear mixed-effects regression	Within $\pm$6 h of peak difference
RETi – NCC	Mean RETi	Large Protected Mature Forest	Site type: Agriculture, Restoration, Paired Forests, Residential*		Welch's ANOVA	Daytime (11 am – 7 pm)
	SD of 24-h mean RETi	Large Protected Mature Forest	Site type (as above)		One-way ANOVA	Daytime (11 am – 7 pm)
	Mean RETi	Smaller Paired Mature Forest	Years since restoration (discrete variable)	Size, site name	Linear mixed-effects regression	Daytime (11 am – 7 pm)

* Suburban residential sites only included for TRCA group of sites.

RLST to decrease with time since restoration. Time from peak RLST difference was included in the linear mixed effects model as we expected the RLST difference to be smaller in the morning and evening. To create a presumed linear relationship, time from peak difference was measured equally in both 'directions' so that if peak was at 13:00, then 12:00 and 14:00 are both counted as the same time (1 h) from peak. The time of peak difference was determined based on spline regression curves fit to the grouped restoration site RLST data. Size of the restoration field was included as larger sites may be less affected by temperature, shading and colonization from the surrounding landscape matrix than smaller sites with less interior core and more edge (Tuff et al., 2016). We used the Kenward-Rogers degrees of freedom method and computed the conditional R^2 for the full model, and marginal R^2 for fixed effects only (Nakagawa and Schielzeth, 2013). Assumptions for the model were tested through visual inspection of diagnostic plots, as recommended in (Zuur et al., 2009).

2.4.2. Analysis of difference in RETi

Analysis of RETi followed the same methods as the RLST analyses described above, although only for the NCC group of sites. Due to overall fewer ET data products available ($n = 9$), and because all were captured during summer daytime (11 to 19 EDT), we included all image products in comparisons of difference in RETi between site types. For visualizations we used a cubic regression as it fit the data best compared to other linear models or spline models, but it was not used beyond visualization.

Welch's corrected ANOVA was applied to RETi data to establish differences between mean RETi of site types (agriculture, restoration, smaller mature forests). We also compared the standard deviation in RETi for each site type through a one-way ANOVA.

We compared RETi for restoration sites by years since restoration. RETi was plotted by diurnal time, with sites clustered into three categories based on "years since restoration began": 1–5 year, 6–9 year, and 10–14 years. The data was then fit to cubic regression curves. To model the change in RETi with time since restoration we fit a linear mixed effects model to test the relationship between RETi and years since restoration (as a discrete variable) and again used site as a grouping factor (random effect).

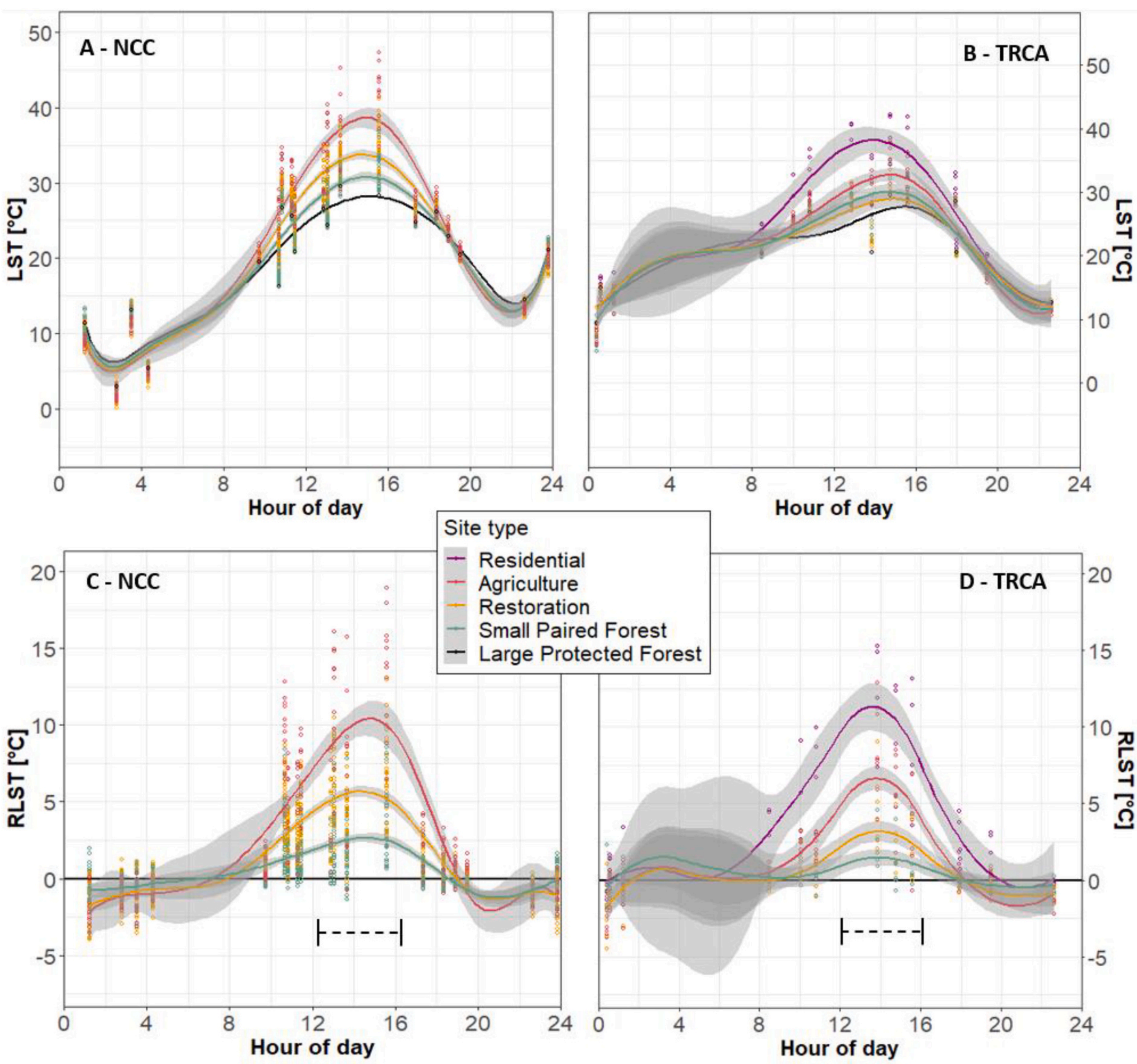

Fig. 3. Land surface temperature (LST) in the NCC (A) and TRCA groups of sites ordered by time of day and grouped by site type, and relative land surface temperature (RLST), relative to the temperature of the large, protected reference forest site in the same image (black x-axis zero line) for the same groups of sites (C and D). Horizontal dashed brackets in C and D indicate period of peak difference. Cubic spline linear regression added for visualization purposes only. The 95% confidence level of the standard error is provided as shading around each curve.

3. Results

3.1. Difference in diurnal RLST dynamics

3.1.1. RLST by site type

LST shows an overall increase in temperature towards mid-afternoon, decreasing into evening as expected (Fig. 3A and B). However, there are data points which deviate from expected diurnal changes, but these may be explained by seasonal, weather, and view angle differences at different dates. One of the more obvious ones is the relatively high temperatures (~20 °C) at 23:48 (image taken on July 27th) for the NCC group of sites compared to overall lower temperatures at 22:37 (image taken September 14th).

All site types in both the TRCA and NCC groups of sites show an increase in RLST (i.e., a decrease in thermal buffering) when compared to the large mature protected forests (x-axis zero line in Fig. 3) over the day. RLST of all site types rise from the morning, peaking in early afternoon and subsequently decreasing towards the evening. The NCC restoration sites' spline regression curve peaked in difference from the Backus Woods forest at 14:15 (Fig. 3C). The RLST of agriculture sites appears to peak later in the day than other site types in the NCC sites, but this pattern is not apparent for TRCA agriculture sites.

With the peak period set for 12:15 to 16:15 EDT (14:15 ± 2 h), four ECOSTRESS thermal images were included for the NCC sites. RLST of sites types were found to be statistically significantly different (ANOVA; $F(2,98.0) = 61.5$, $p < 0.001$, adjusted $R^2 = 0.38$). All site types were statistically distinct from each other as per *post-hoc* testing. Agricultural fields had the highest mean RLST within the 4 h peak period of 9.8 °C above that of the large mature forest site. Restoration fields had a mean peak period temperature of 5.4 °C. Mature forests had the lowest peak period RLST of 2.5 °C (see Appendix C for data tables).

The results from the TRCA group of sites were in large part similar to those of the NCC group of sites. The TRCA restoration sites had the highest mean RLST compared to the protected mature Albion Hills forest near 14:05 EDT as per the spline regression (Fig. 3D). Period of peak difference for the TRCA group was therefore set to 12:05 to 16:05 EDT (14:05 ± 2 h) for the ANOVA. Three ECOSTRESS thermal images were within this time-span and therefore included in the two-way fixed ANOVA of peak period RLST difference. There was a significant difference in mean RLST by site type ($F(3,62) = 36.1$, $p < 0.001$) and by image ID ($F(2, 62) = 9.2$, $p < 0.001$) for the TRCA sites. No statistical difference was detected based on the 'site type by image ID' interaction term ($F(6, 62) = 0.6$, $p = 0.725$, adjusted $R^2 = 0.62$) in the same test. Residential sites had the highest mean peak RLST (10.3 °C), followed by agricultural fields (5.9 °C). Restored fields and mature forests had the lowest mean peak RLST of 2.9 °C and 1.3 °C, respectively (see Appendix C for data tables).

Standard deviation in RLST over the full 24-h cycle of NCC sites differed significantly among site types (ANOVA; $F(2,82) = 65.3$, $p < 0.001$), and each pair-wise difference was also significant (Fig. 4A). Standard deviation in RLST was highest for agriculture fields (mean SD = 5.16 °C), lowest for forest sites (mean SD = 1.69C°), and intermediate for the restoration sites (mean SD = 2.89 °C).

RLST differed significantly between site types for the TRCA sites (ANOVA; $F(3,23) = 15.2$, $p < 0.001$). For the TRCA sites, *post-hoc* testing identified no statistically significant differences between restoration and forest sites, or between residential sites and agriculture sites. However, significant differences were found between all other site pair-wise comparisons, notably between agricultural sites and restoration sites. The standard deviation of RLST was highest for residential sites (mean SD = 4.30 °C) and agriculture sites (mean SD = 3.25C°), and lowest for restoration sites (mean SD = 1.99C°) and forest sites (mean SD = 0.82C°; Fig. 4B). Site "MF5728" was removed from the TRCA site analysis of standard deviation as the Dixon test registered its standard deviation temperature result as an outlier. The removed site was located in the smallest forest and surrounded by active agricultural fields.

3.1.2. Modeling change in RLST by years since restoration

RLST of all age-grouped NCC restoration sites peak near 14:00 EDT and decline towards night-time as per their spline regression curves (Fig. 5A), although older restoration sites appear to have lower peaks relative to younger sites. Fewer overall sites, and only one site in the 1–5 year age group increased confidence intervals of the spline regression curve for the TRCA sites (Fig. 5B), as compared to the NCC sites. The peak of RLST difference for TRCA sites, averaged by age-group, was at approximately 13:00 EDT (Fig. 5). There is no apparent shift in peak time with restoration age-group for the either group of sites.

We found a significant decrease in mean daytime RLST of −0.1C° per

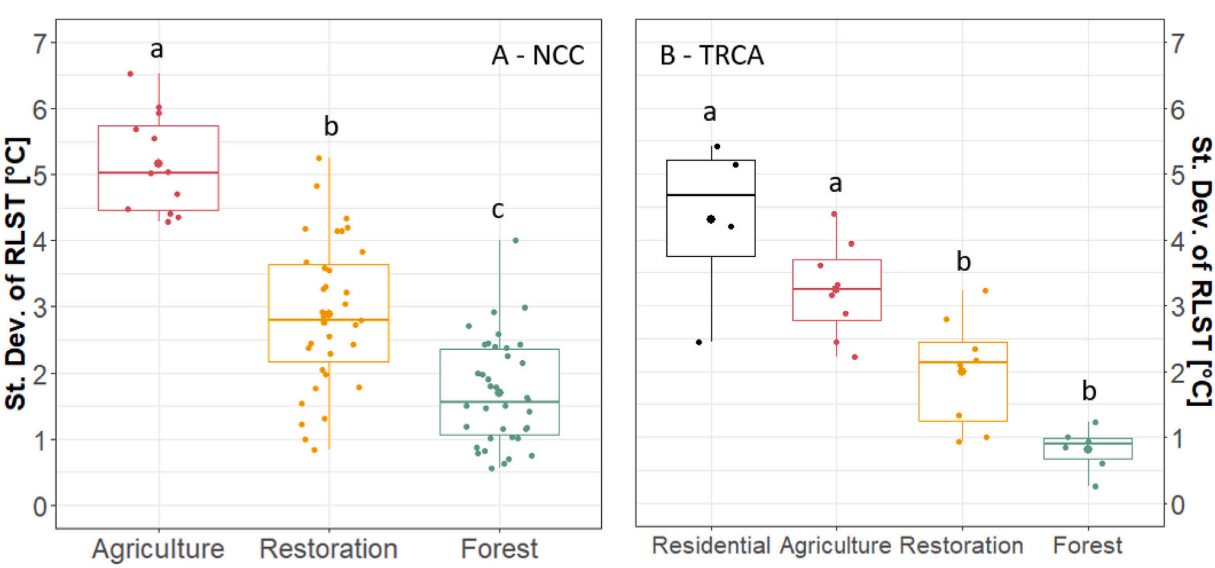

Fig. 4. Boxplot of the standard deviation of the relative land surface temperature (RLST) of each site type in the NCC and TRCA group of sites relative to the LST of the Backus Woods (NCC) or Albion Hills (TRCA) large mature protected reference forest (x-axis zero-line) over the full 24-h cycle. Boxes represent quartiles of the data, whiskers represent 1.5 interquartile range from nearest quartile, or most extreme value, whichever is shortest. Horizontal line in box represents median and larger dot represents mean. Points for sites are jittered for easier viewing. Letters indicate significant difference ($p < 0.05$) as per Tukey-adjusted pairwise post hoc test.

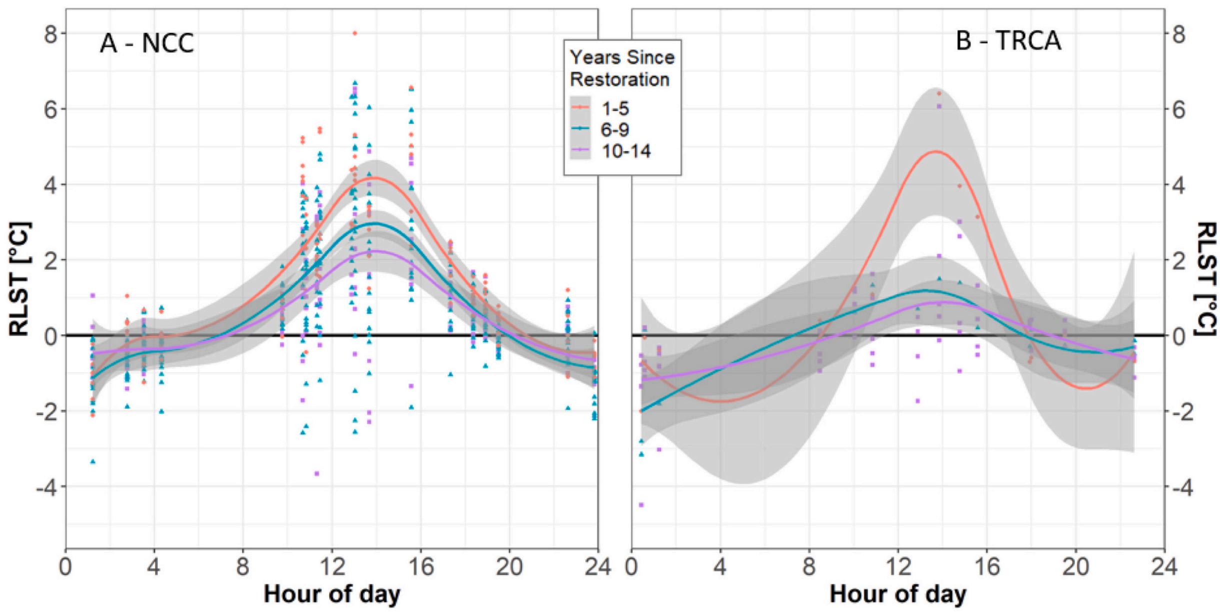

Fig. 5. Mean relative land surface temperature (RLST) of restoration sites relative to the mean temperature of their paired mature reference forest sites (represented by the x-axis zero-line) over time of day for the (A) NCC group and (B) TRCA group. A cubic spline regression curve has been fitted for three groups of restoration ages. The 95% confidence level of the standard error is provided as shading around each curve. The NCC group has 8 fields 1–5 years old, 20 fields 6–9 years, and 7 fields 10–14 years. TRCA has 1 field 1–5 years, 2 fields 6–9 years and 5 fields 10–14 years.

year since restoration for the NCC group of restoration sites as determined by the linear mixed effects regression ($p = 0.038$, Table 3). There was also a significant effect of restoration area size, and hours from 14:00 peak. The model has a marginal R^2 of 0.37, meaning that the fixed independent factors explained more than a third of the variation in the data. The relative difference in LST between NCC restoration sites of 1 to 5 years, and their paired mature forests, for the hours studied, was between 1 and 4 °C. Assuming a continued linear decrease of 0.1C°/year, and a mean daytime RLST difference of 3 °C, the restoration sites would reach the same daytime surface temperatures as their paired mature forest sites in approximately 32 years (3.1% change per year).

For the TRCA group of restoration sites' linear mixed effects regression, peak time was identified as 1 pm (Table 4). Statistically significant decreases in RLST were found based on hours from 1 pm peak and from restoration area size. However, no significant change in RLST on years since restoration was found.

Table 3
Linear mixed-effects model with daytime relative land surface temperature (RLST) of NCC restoration sites relative to the mean surface temperature of paired mature reference forest site as dependent variable. Years since restoration, size of restoration area (ha) and hours from 14 EDT peak as fixed effect independent variables. Restoration site is used as random effect grouping factor. DF. (K-R) – Degrees of Freedom, Kenward-Roger estimation method. Marginal-R^2 includes fixed effects only, Conditional R^2 include all factors. Significant (95% CI) *p*-values bolded.

	RLST (C°)				
	Coefficient	Std. error	DF. (K-R)	t-value	*p*-value
Years Since Restoration	−0.094	0.043	29.8	−2.170	**0.038**
Restoration area size (ha)	0.067	0.020	30.6	3.263	**0.002**
Hours from 14 EDT peak	−0.605	0.040	30.6	−15.154	**<0.001**
Constant	3.319	0.500	34.1	6.635	**<0.001**
Observations (fields)	402 (35)				
Marginal/ Conditional R^2	0.37/0.57				

Table 4
Linear mixed-effects model with relative land surface temperature (RLST) of TRCA restoration sites relative to the mean surface temperature of paired mature reference forest site as dependent variable. Years since restoration, size of restoration area (ha) and hours from 13 EDT peak as fixed effect independent variables. Restoration site is used as random effect grouping factor. DF. (K-R) – Degrees of Freedom, Kenward-Roger estimation method. Marginal-R^2 includes fixed effects only, Conditional R^2 include all factors. Significant (95% CI) *p*-values bolded.

	RLST (C°)				
	Coefficient	Std. error	DF. (K-R)	t-value	*p*-value
Years Since Restoration	−0.001	0.902	5.8	−0.602	0.994
Restoration area size (ha)	0.167	0.048	5.8	1.677	**0.024**
Hours from 13 EDT peak	−0.411	0.107	5.8	−7.038	**<0.001**
Constant	0.767	0.106	5.8	1.902	0.434
Observations (fields)	54 (7)				
Marginal/Conditional R^2	0.37/0.38				

3.2. Difference in diurnal RETi dynamics

3.2.1. RETi by site type

Absolute ETi decreased from a peak mean of approximately 300 W/m^2 at mid-day (11:30 to 13:40 EDT), to approximately 100 W/m^2 in the late afternoon/evening (17:10 to 19:00) (Fig. 6A). The NCC sites were consistently cloudy in the morning at the time of ISS/ECOSTRESS flyover (prior to 11:00), resulting in no cloud-free data to extend the diurnal curves. RETi appears to increase for all site types over time of day from before noon to late afternoon (Fig. 6B). The adjusted R^2 of the cubic regression of RETi over time of day was 0.39, this was also unchanged when including site type.

We found a significant difference in mean RETi between site-types (ANOVA; $F(2, 252) = 3.14$, $p = 0.045$). However, the adjusted R^2 of 0.01 indicated that negligible variability was accounted for in this model. Because of the very low R^2, we did not perform further post-hoc

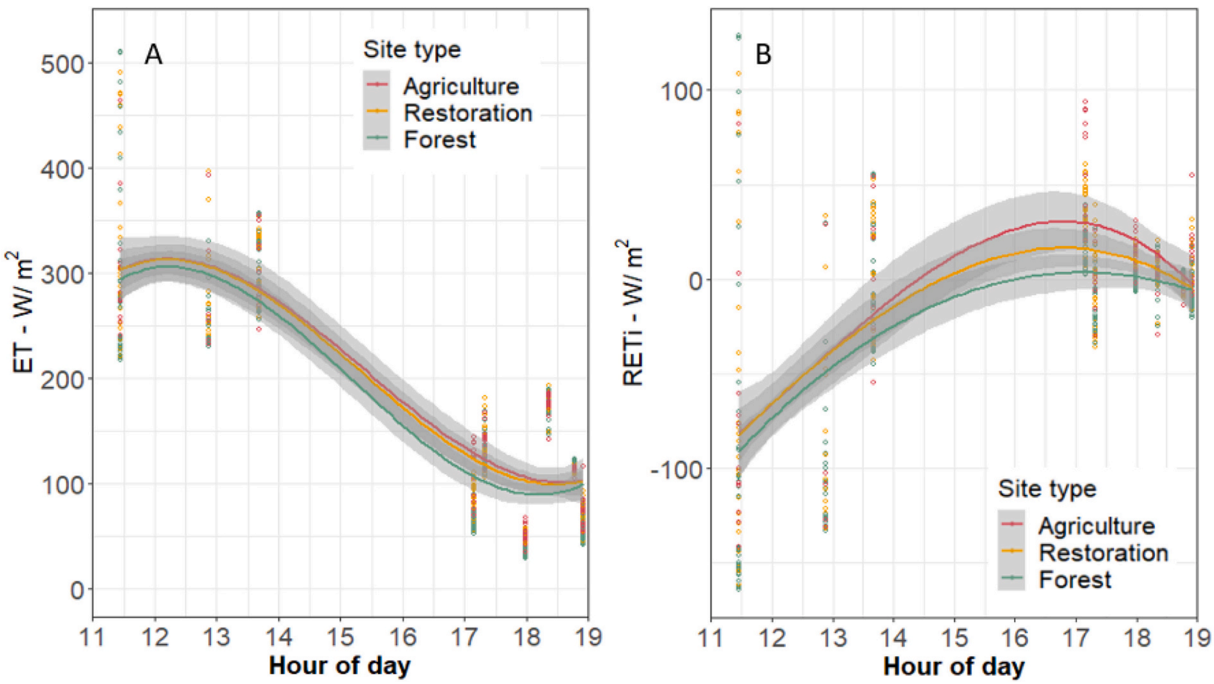

Fig. 6. Cubic regression of (A) absolute instantaneous ET and (B) relative instantaneous ET (RETi) of sites in the NCC group. For B, RETi was calculated against the ET of the large, protected Backus Woods reference forest site in the same image. The 95% confidence level of the standard error is provided as shading around each curve.

testing.

We found no significance in the standard deviation of RETi (between 11:00 and 19:00) between site types (ANOVA; $F(2,79) = 0.09$, $p = 0.909$). The mean standard deviation of RETi varied by 45–50 W/m^2 more for all site types (Fig. 7) as compared to that of the large, protected forest (Backus Woods).

3.2.2. Modeling change in RETi by years since restoration

Visually the RETi of restoration sites grouped by age appeared to fall into two patterns: observed RETi of restoration sites 6–9 and 10–14 years since restoration, had a mean within 10 W/m^2 of their paired forest area throughout the diurnal period, while sites 1–5 years old had a higher and more varied RETi. The RETi of the youngest group of sites had means ranging from 5 to 25 W/m^2 above that of their paired restoration site (Fig. 8).

RETi decreased significantly ($t = -3.66$, $p < 0.001$) by an average of 0.8 W/m^2 in instantaneous ET continuously throughout summer daytimes per year since restoration, as established by the linear mixed effects model (Table 5). RETi also increased significantly with the size of the restoration site. This model had a marginal R^2 of 0.11. The RETi difference between the youngest restoration sites and their paired forest sites were on average 12.3 W/m^2 throughout the day. A 0.8 W/m^2 (instantaneous) per year change then represents a 6.3% change, or approximately 16 years to reach ET levels of the forests. However, because of the relatively lower marginal R^2, RETi results should be interpreted with some caution.

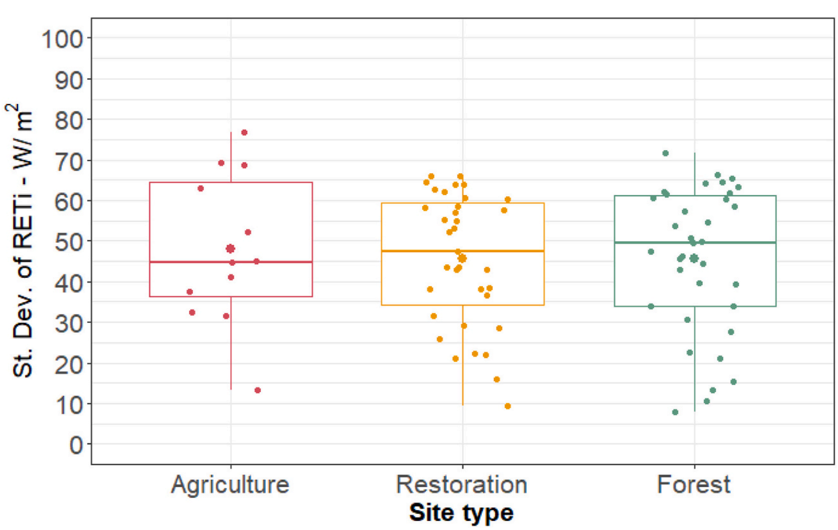

Fig. 7. Boxplot of the standard deviation of RETi of each site type in the NCC group of sites relative to the ETi of the Backus Woods large mature protected reference forest (x-axis zero-line) over the full 24-h cycle. Boxes represent quartiles of the data, whiskers represent 1.5 interquartile range from nearest quartile, or most extreme value, whichever is shortest. Horizontal line in box represents median and larger dot represents mean. Points for sites are jittered.

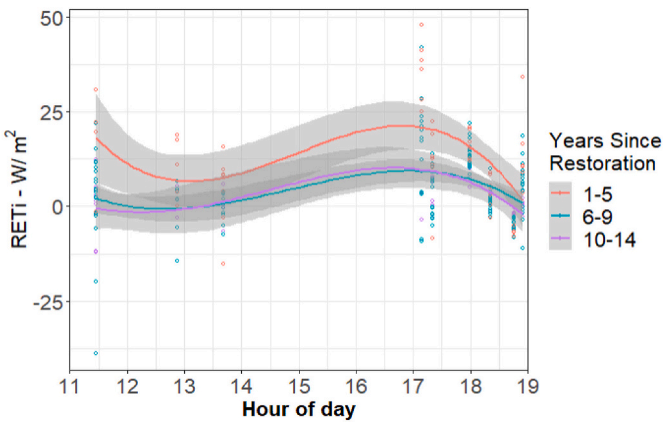

Fig. 8. Mean paired RETi of restoration sites, relative to ETi of paired reference forests, over time of day for the NCC group of sites. To help visualization a cubic regression curve has been fitted for three groups of restoration ages. The 95% confidence level of the standard error is provided as shading around each curve. There were 8 fields 1–5 years old, 20 fields 6–9 years, and 7 fields 10–14 years.

Table 5
Linear mixed-effects model of paired RETi of restoration sites as dependent variable. Years since restoration and size of restoration area (ha) as fixed effect independent variables. Restoration site is used as random effect grouping factor. DF. (K-R) – Degrees of Freedom, Kenward-Roger estimation method. Marginal-R^2 includes fixed effects only, Conditional R^2 include all factors. Significant (95% CI) p-values bolded.

	RETi – W/m^2				
	Coefficient	Std. error	DF. (K-R)	t-value	*p*-value
Years Since Restoration	−0.784	0.214	41.9	−3.657	**<0.001**
Restoration area size (ha)	0.257	0.103	43.2	2.502	**0.016**
Constant	7.682	2.393	42.1	3.210	**0.002**
Observations (fields)	241 (35)				
Marginal/Conditional R^2	0.11/0.16				

4. Discussion

4.1. Differences in thermal buffering by land cover

The increase in thermal buffering capacity of forested relative to non-forested sites was most pronounced between 12 and 16 local time, peaking around 14. Assuming no water stress, relative ET capacity and physical heat storage of forests are expected to be greatest and to provide the most cooling at this time in the afternoon (Meier et al., 2019; Xiao et al., 2021). We did not identify any noticeable shifts in the time of diurnal peak thermal buffering for different land covers or time since restoration, in contrast to what has been hypothesized due to increased physical and chemical heat storage (Ulanowicz and Hannon, 1987).

Temperate forests have been found to reduce diurnal variation of temperature when compared to other land cover on a global scale with coarse spatial resolution satellites (Meier et al., 2019) and when measured locally on the ground with thermometers in a forest (Chen et al., 1999). Similarly, we found that our forest sites, measured through moderate resolution imagery, had the lowest diurnal land surface temperature (LST) variation, relative to the other land cover classes examined. If not restored, a common fate for agriculture sites near cities are to be developed into low-density residential areas (Cramer et al., 2008). Our results show that these residential developments of agriculture would shift LST of formerly agricultural lands towards more extremes. Suburban residential sites generally have lower plant biomass, diversity, and complexity. Heat is also added through energy consumption of buildings and traffic and the emissivity and albedo of roofs and paved surfaces. Quantifying the difference and pace of change in thermal buffering capacity between forest restoration sites and suburban residential sites can inform and guide decision-makers and planners who are deciding the future of former agricultural lands.

The goal of the active forest restorations studied was to facilitate the transition of former agriculture sites to forest, and its success is determined by changes in function, structure, and diversity (Reif and Theel, 2017). In this study, restoration sites were found to have a LST variation in between that of forest and agriculture sites. In conjunction with the result that daytime relative LST (RLST) decreased with years since restoration for the NCC group of sites, the relatively lower standard deviation of RLST indicates that restoration sites are becoming more like mature deciduous forests. Diurnal RLST variation therefore appears useful as a measurement of the trajectory and pace of forest recovery after restoration. Temperature regulation and thermal buffering has mainly been considered an ecosystem service in urban settings, as it benefits human well-being (Gómez-Baggethun and Barton, 2013). However, the thermal buffering effects of forest restoration in rural settings can also be considered a regulating and supporting ecosystem service that benefits ecosystem function (e.g., improved water quality due to forest stream temperature) and forest habitat, which in turn benefits biodiversity. Thermal buffering should be considered in addition to the other ecosystem services which forest restoration can provide, such as habitat creation and carbon sequestration (Bullock et al., 2011).

4.2. Reduction in daytime temperature with restoration

Given observed decreases in RLST in response to time since restoration, restoration sites in the NCC group are likely to reach the same LST as a mature reference forest ecosystem in the same area after approximately 32 years. Decades-old NCC restoration sites have already achieved near complete canopy cover, while others are expected to reach it in at most another 10 years. In red oaks (*Quercus rubra*), a commonly seeded and planted tree in both groups of restoration sites, sexual maturity (i.e., acorn production) typically occurs after 30–50 years while reaching full size takes longer (50–100 years) (Kormanik et al., 2004). We may therefore expect that the decrease of daytime LST will continue, although this rate of increase will likely slow as canopy closure occurs. This trend would be in line with other studies which have found a continued decrease in air-temperature in and above forest canopy for forests older than 40 years (Lin et al., 2017; Norris et al., 2012).

Variation in RLST of the TRCA restoration sites was intermediate between that of the agricultural and forested sites. However, in contrast to our expectations, we were not able to identify any significant decrease in RLST as a function of time since restoration was initiated for the TRCA sites. One possible explanation of this result is that the TRCA sites were too small, too few, or with not enough difference in ages, to be accurately measured using ECOSTRESS. TRCA sites had a median size of 3.8 ha vs. 10 ha for the NCC sites and covered a shorter span of years since restoration than the NCC sites. The difference in results between the two groups of sites could also be due to differences in restoration methods (e.g., site preparation, planting strategies and species composition) or site conditions (e.g., soil properties and water tables). Future work should examine explicitly differences in the rates of change in restorations sites as a function of the different planting strategies employed.

RLST increased with restoration site size at both the TRCA and NCC sites. Noting that the majority of restoration sites primarily bordered forest, an explanation for this RLST increase with size may be that larger sites have a larger hotter core area located further away from surrounding forest edge, even when taking into account the 50 m internal buffer (Tuff et al., 2016). Smaller sites surrounded by forests may also be colonized more rapidly by surrounding vegetation (Brunet et al., 2012), which would also increase the cooling rate.

4.3. Difference in ET by land cover and with restoration

We found that the most recently restored sites (1–5 years) in the NCC group had the highest daytime temperatures while also appearing to have the highest RETi. With the rate of change in the model, the restoration sites would take an approximately 20 years to reach the ET levels of the mature reference forest sites. Older restoration sites are more similar to the mature forest sites in terms of rate of ET, and may be more able to control their water usage through plant transpiration and the closing of leaf stomata during times of extreme heat (Bonan, 2008). However, the variance captured by the model comparing RETi by years since restoration was low (marginal $R^2 = 0.11$), and we did not find a substantial difference in either mean or diurnal standard deviation of RETi for different land cover types. Improvements in the ECOSTRESS ET algorithm or its inputs may be required to compare ET of land cover types. Current additional inputs for the ET algorithm come from Landsat, MODIS and/or weather stations. These are limited by overlap in overpass time, spatial resolution, or the accuracy of spatial scaling. Utilizing data from planned satellite imaging platforms that combine moderate resolution multi-band thermal imagers, such as NASA SBG would reduce this need for overlapping additional inputs (Germain et al., 2021). Southern Ontario is a relatively cloudy region, as compared to the ECOSTRESS testing site of Southern California (Hook et al., 2019). This reduces the amount of useable imagery. Increasing the amount of imagery captured by more platforms would improve both the number of cloud-free images captured, and the overlap with other imagers needed for ET calculations.

Although our findings regarding ET are less robust than those for RLST, they are nonetheless qualitatively in agreement with other studies of ET dynamics in forest ecosystems. For example, (Naranjo et al., 2012) found that ET rates increased for the first 5–10 years following logging due to evaporation from bare soil. The apparent disconnect between LST and ET may be explained by the ecology of older restoration sites, in that they have higher physical heat capacity in the woody structure of trees and shrubs and in the water contained in leaves and stems (Meier et al., 2019). Vegetation of more developed ecosystems may also thermoregulate through emissivity, albedo, and other trait-related changes (Michaletz et al., 2015). Looking at relative ET of restoration sites 6–9 and 10–14 years, the difference appears to be small, if any. Older but still well-documented restoration projects need to be studied in order to quantify ET change with restoration over a longer timespan using ECOSTRESS or similar instruments.

4.4. Applications in ecology and restoration

Further studies are needed to determine the connection between diurnal LST variation and thermal buffering and different ecological attributes. LST and its variation is tied to ecosystem energy reflection, conversion, and storage (Hamberg et al., 2020; Meier et al., 2019; Norris et al., 2012), but which attributes (e.g., biomass, diversity, albedo, root depth) have the most impact on LST at different times of the day remains to be studied. One approach to study these connections would be to image experimental forest plots with fixed variation of ecosystem attributes, such as those of the IDENT sites (Tobner et al., 2014), using drone-borne or tower-based thermal imagers with high temporal resolution. Another approach is to use larger natural experiments, in the form of restoration projects, where site factors vary but restoration methods stay constant, or vice versa. These natural experiments could be studied, for example, by comparing ECOSTRESS data with data from other ISS instruments, such as estimations of CO_2 from OCO-3 and forest structure measurements from the GEDI LiDAR (Stavros et al., 2017). Combining ISS instruments' data would ensure complete spatio-temporal overlap when studying the connection between LST and ET dynamics with ecosystem attributes at restoration sites.

Lack of cost-effective and accurate monitoring methods is an ongoing and urgent issue for ecosystem restoration (DeLuca et al., 2010; Reif and Theel, 2017). For large, remote, or geographically scattered restoration sites monitoring on the ground (by trained ecologists, flux towers, or other methods) may not be possible, due to lack of funding or access. In these cases, ECOSTRESS and similar moderate resolution thermal imaging instruments could be powerful monitoring tools (Anderson et al., 2021; Hulley et al., 2019). Remote thermal monitoring could identify restoration sites that are slow to cool or buffer diurnal temperature, where recovery may have been impaired by issues such as drought, pests, disease, or a mismatch between seeds/planting stock and site conditions (Chen et al., 1999; Hamberg et al., 2020). From the findings in this study, and the statistically non-significant results from the smaller TRCA sites in terms of temperature change over time since restoration and ET change, a rule of thumb for a "large enough" restoration site for current moderate resolution thermal imaging may be at least 5 ha, rather than 2 ha used in this study. Part of the need for larger minimum size of sites, or finer resolution instruments, is the effect of relatively large zenith view angles, which lead to coarser spatial resolution (Xue et al., 2020).

Efforts to sharpen the resolution of ECOSTRESS (e.g., Xue et al., 2020) could potentially decrease the minimum size of restoration sites that could be studied. Coordination of orbit and coverage of ECOSTRESS with upcoming platforms including SBG, TRISHNA, Copernicus ESA-LSTM, and ASI-Platino+, could increase temporal resolution as well (Germain et al., 2021). From a restoration ecology perspective, to operationalize thermal and ET measures from ECOSTRESS and similar instruments, the image products need to be provided pre-processed, and in a format where restoration managers can compare data over time for their sites in an intuitive and user-friendly interface. Similar requirements would be needed to operationalize ECOSTRESS data for measuring thermal buffering as an ecosystem service provided by restoration. The relative upside, compared to agricultural or fire monitoring, is that due to the relatively slow process of restoration, data would not have to processed rapidly or provided daily. A seasonal report of relative temperature and ET change may be all a manager needs. Such a report could be used to communicate thermal buffering gains to funders and the public in order to garner further support. These reports could also be used to prioritize which sites need to be visited by trained staff to diagnose why there is lack of thermal buffering or ET change. This diagnosis would then be used to determine how management may need to be adapted (e.g., through pesticide spraying, re-planting, herbivory fencing). This approach would in many cases be a big step up from very little, to no long-term monitoring at all, which is the current reality for many forest restoration projects (DeLuca et al., 2010; Reif and Theel, 2017).

CRediT authorship contribution statement

L. Jonas Hamberg: Conceptualization, Methodology, Data curation, Formal analysis, Investigation, Writing – original draft, Writing – review & editing, Visualization. **Joshua B. Fisher:** Conceptualization, Methodology, Writing – review & editing. **Jonathan L.W. Ruppert:** Conceptualization, Methodology, Writing – review & editing, Supervision, Funding acquisition. **Jessica Tureček:** Methodology, Writing – review & editing, Formal analysis. **Dean H. Rosen:** Data curation, Visualization. **Patrick M.A. James:** Conceptualization, Methodology, Writing – review & editing, Supervision, Funding acquisition.

Declaration of Competing Interest

The authors declare that they have no known competing financial interests or personal relationships that could have appeared to influence the work reported in this paper.

Acknowledgements

JH was supported through a postdoctoral fellowship funded by Mitacs and the Toronto and Region Conservation Authority (TRCA). JBF was supported by NASA's ECOSTRESS. We would like to acknowledge the help from Nature Conservancy of Canada (NCC) southern Ontario staff, including Liv Monck-Whipp, for access to NCC site data. Thanks to Michael McTavish for reviewing the statistical methods used and to Harshita Yalamarty for copy editing. Thanks to TRCA Restoration and GIS staff for providing background data.

Appendix A. Supplementary data

Supplementary data to this article can be found online at https://doi.org/10.1016/j.rse.2022.113178.

References

Aires, F., Prigent, C., Rossow, W.B., 2004. Temporal interpolation of global surface skin temperature diurnal cycle over land under clear and cloudy conditions. J. Geophys. Res.-Atmos. 109.

Anderson, M.C., Yang, Yang, Xue, J., Knipper, K.R., Yang, Yun, Gao, F., Hain, C.R., Kustas, W.P., Cawse-Nicholson, K., Hulley, G., 2021. Interoperability of ECOSTRESS and Landsat for mapping evapotranspiration time series at sub-field scales. Remote Sens. Environ. 252, 112189.

Baldocchi, D.D., 2005. The role of biodiversity on the evaporation of forests. In: Forest Diversity and Function. Springer, pp. 131–148.

Bonan, G.B., 2008. Ecological Climatology: Concepts and Applications. Cambridge University Press, Cambridge, UK.

Broadhurst, L.M., Jones, T.A., Smith, F.S., North, T.O.M., Guja, L., 2016. Maximizing seed resources for restoration in an uncertain future. BioScience 66, 73–79.

Brunet, J., De Frenne, P., Holmström, E., Mayr, M.L., 2012. Life-history traits explain rapid colonization of young post-agricultural forests by understory herbs. For. Ecol. Manag. 278, 55–62.

Bullock, J.M., Aronson, J., Newton, A.C., Pywell, R.F., Rey-Benayas, J.M., 2011. Restoration of ecosystem services and biodiversity: conflicts and opportunities. Trends Ecol. Evol. 26, 541–549. https://doi.org/10.1016/j.tree.2011.06.011.

Cai, Z., Jönsson, P., Jin, H., Eklundh, L., 2017. Performance of smoothing methods for reconstructing NDVI time-series and estimating vegetation phenology from MODIS data. Remote Sens. 9, 1271.

Cai, Y., Chen, Y., Tong, C., 2019. Spatiotemporal evolution of urban green space and its impact on the urban thermal environment based on remote sensing data: a case study of Fuzhou City, China. Urban For. Urban Green. 41, 333–343.

Chen, J., Saunders, S.C., Crow, T.R., Naiman, R.J., Brosofske, K.D., Mroz, G.D., Brookshire, B.L., Franklin, J.F., 1999. Microclimate in forest ecosystem and landscape ecology: variations in local climate can be used to monitor and compare the effects of different management regimes. BioScience 49, 288–297.

Chen, J.M., Deng, F., Chen, M., 2006. Locally adjusted cubic-spline capping for reconstructing seasonal trajectories of a satellite-derived surface parameter. IEEE Trans. Geosci. Remote Sens. 44, 2230–2238.

Cramer, V.A., Hobbs, R.J., Standish, R.J., 2008. What's new about old fields? Land abandonment and ecosystem assembly. Trends Ecol. Evol. 23, 104–112.

Curran, C., 2018. A trip back in time: exploring the history of Backus Woods. In: Land Lines: The Nature Conservancy of Canada Blog. URL. https://www.natureconservancy.ca/en/blog/archive/a-trip-back-in-time.html#.YQRaqI4VaUk.

DeLuca, T.H., Aplet, G.H., Wilmer, B., Burchfield, J., 2010. The unknown trajectory of forest restoration: a call for ecosystem monitoring. J. For. 108, 288–295.

van Dijk, A., Keenan, R.J., 2007. Planted forests and water in perspective. For. Ecol. Manag. 251, 1–9.

Ehbrecht, M., Schall, P., Ammer, C., Fischer, M., Seidel, D., 2019. Effects of structural heterogeneity on the diurnal temperature range in temperate forest ecosystems. For. Ecol. Manag. 432, 860–867.

Elsen, P.R., Farwell, L.S., Pidgeon, A.M., Radeloff, V.C., 2020. Landsat 8 TIRS-derived relative temperature and thermal heterogeneity predict winter bird species richness patterns across the conterminous United States. Remote Sens. Environ. 236, 111514.

Environment Canada, 2021. Historical Data - Climate - Environment and Climate Change Canada [WWW Document]. URL. http://climate.weather.gc.ca/historical_data/search_historic_data_e.html (accessed 2.4.22).

Esri, DigitalGlobe, GeoEye, i-cubed, USDA FSA, USGS, AEX, Getmapping, Aerogrid, IGN, IGP, swisstopo, GIS User Community, 2021. World Imagery [WWW Document]. URL. https://www.arcgis.com/home/item.html?id=10df2279f9684e4a9f6a7f08febac2a9.

Filoso, S., Bezerra, M.O., Weiss, K.C., Palmer, M.A., 2017. Impacts of forest restoration on water yield: a systematic review. PLoS One 12, e0183210.

Fisher, J.B., Whittaker, R.J., Malhi, Y., 2011. ET come home: potential evapotranspiration in geographical ecology. Glob. Ecol. Biogeogr. 20, 1–18.

Fisher, J.B., Melton, F., Middleton, E., Hain, C., Anderson, M., Allen, R., McCabe, M.F., Hook, S., Baldocchi, D., Townsend, P.A., 2017. The future of evapotranspiration: global requirements for ecosystem functioning, carbon and climate feedbacks, agricultural management, and water resources. Water Resour. Res. 53, 2618–2626.

Fisher, J.B., Lee, B., Purdy, A.J., Halverson, G.H., Dohlen, M.B., Cawse-Nicholson, K., Wang, A., Anderson, R.G., Aragon, B., Arain, M.A., 2020. ECOSTRESS: NASA's next generation mission to measure evapotranspiration from the international Space Station. Water Resour. Res. 56, e2019WR026058.

U.S. Geological Survey, 2016. Landsat—Earth Observation Satellites (No. Fact Sheet 2015-3081). U.S. Geological Survey.

Germain, K.St., Schimel, D., Poulter, B., 2021. SBG Community Webinar 4 [WWW Document]. URL. https://sbg.jpl.nasa.gov/doc_links/2021-02-18-sbg-community-webinar-4.

Gianinetto, M., Villa, P., 2007. Rapid response flood assessment using minimum noise fraction and composed spline interpolation. IEEE Trans. Geosci. Remote Sens. 45, 3204–3211.

Giglio, L., 2007. Characterization of the tropical diurnal fire cycle using VIRS and MODIS observations. Remote Sens. Environ. 108, 407–421.

Gómez-Baggethun, E., Barton, D.N., 2013. Classifying and valuing ecosystem services for urban planning. Ecol. Econ. 86, 235–245.

Hamberg, Jonas, 2022. Datasets for: Assessing and modeling diurnal temperature buffering and evapotranspiration dynamics in forest restoration using ECOSTRESS thermal imaging. Mendeley Data, V1. https://doi.org/10.17632/7cy3235pkj.1.

Hamberg, L.J., Fraser, R.A., Robinson, D.T., Trant, A.J., Murphy, S.D., 2020. Surface temperature as an indicator of plant species diversity and restoration in oak woodland. Ecol. Indic. 113.

Holl, K.D., Brancalion, P.H., 2020. Tree planting is not a simple solution. Science 368, 580–581.

Holmes, T.R.H., Crow, W.T., Hain, C., Anderson, M.C., Kustas, W.P., 2015. Diurnal temperature cycle as observed by thermal infrared and microwave radiometers. Remote Sens. Environ. 158, 110–125.

Hook, S.J., Cawse-Nicholson, K., Barsi, J., Radocinski, R., Hulley, G.C., Johnson, W.R., Rivera, G., Markham, B., 2019. In-flight validation of the ECOSTRESS, Landsats 7 and 8 thermal infrared spectral channels using the Lake Tahoe CA/NV and Salton Sea CA automated validation sites. IEEE Trans. Geosci. Remote Sens. 58, 1294–1302.

Hulley, G., Freepartner, R., 2019. ECOsystem Spaceborne Thermal Radiometer Experiment on Space Station (ECOSTRESS) Mission - Level 2 Product User Guide (No. JPL D103137 Version 2). Jet Propulsion Laboratory, California Institute of Technology.

Hulley, G.C., Ghent, D., Hook, S.J., 2019. A look to the future: thermal-infrared missions and measurements. In: Taking the Temperature of the Earth. Elsevier, pp. 227–237.

Hunting Survey Corporation Limited, 1954. Digital Aerial Photographs, Southern Ontario 1954 [WWW Document]. URL. https://mdl.library.utoronto.ca/collections/air-photos/1954-air-photos-southern-ontario/index (accessed 6.3.20).

Kormanik, P.P., Sung, S.-J.S., Kormanik, T., Tibbs, T., Zarnoch, S.J., 2004. Northern Red Oak from Acorns to Acorns in 8 Years or Less. Gen. Tech. Rep. SRS–71. US Department of Agriculture, Forest Service, Southern Research Station, Asheville, NC.

Lin, H., Fan, Z., Shi, L., Arain, A., McCaughey, H., Billesbach, D., Siqueira, M., Bracho, R., Oechel, W., 2017. The cooling trend of canopy temperature during the maturation, succession, and recovery of ecosystems. Ecosystems 20, 406–415. https://doi.org/10.1007/s10021-016-0033-8.

Lin, H., Tu, C., Fang, J., Gioli, B., Loubet, B., Gruening, C., Zhou, G., Beringer, J., Huang, J., Dušek, J., 2020. Forests buffer thermal fluctuation better than non-forests. Agric. For. Meteorol. 107994.

Londe, V., Farah, F.T., Rodrigues, R.R., Martins, F.R., 2020. Reference and comparison values for ecological indicators in assessing restoration areas in the Atlantic Forest. Ecol. Indic. 110, 105928.

Meier, R., Davin, E.L., Swenson, S.C., Lawrence, D.M., Schwaab, J., 2019. Biomass heat storage dampens diurnal temperature variations in forests. Environ. Res. Lett. 14, 084026.

Meli, P., Holl, K.D., Rey Benayas, J.M., Jones, H.P., Jones, P.C., Montoya, D., Moreno Mateos, D., 2017. A global review of past land use, climate, and active vs. passive restoration effects on forest recovery. PLoS One 12, e0171368.

Michaletz, S.T., Weiser, M.D., Zhou, J., Kaspari, M., Helliker, B.R., Enquist, B.J., 2015. Plant thermoregulation: energetics, trait–environment interactions, and carbon economics. Trends Ecol. Evol. 30, 714–724.

Nakagawa, S., Schielzeth, H., 2013. A general and simple method for obtaining R2 from generalized linear mixed-effects models. Methods Ecol. Evol. 4, 133–142.

Naranjo, J.A.B., Stahl, K., Weiler, M., 2012. Evapotranspiration and land cover transitions: long-term watershed response in recovering forested ecosystems. Ecohydrology 5, 721–732.

Nature Conservancy of Canada, 2006. Property Management Plan - Lake Erie Farms Property. NCC - Southwestern Ontario Region, London, Ontario.

Norris, C., Hobson, P., Ibisch, P.L., 2012. Microclimate and vegetation function as indicators of forest thermodynamic efficiency. J. Appl. Ecol. 49, 562–570.

Oyoshi, K., 2014. Hourly LST monitoring with Japanese geostationary satellite MTSAT-1R over the Asia-Pacific region. Asian J. Geoinform. 14.

Qiao, Z., Tian, G., Xiao, L., 2013. Diurnal and seasonal impacts of urbanization on the urban thermal environment: a case study of Beijing using MODIS data. ISPRS J. Photogramm. Remote Sens. 85, 93–101.

Reif, M.K., Theel, H.J., 2017. Remote sensing for restoration ecology: application for restoring degraded, damaged, transformed, or destroyed ecosystems. Integr. Environ. Assess. Manag. 13, 614–630.

Ruiz-Jaen, M.C., Aide, T.M., 2005. Restoration success: how is it being measured? Restor. Ecol. 13, 569–577. https://doi.org/10.1111/j.1526-100X.2005.00072.x.

Smyth, M., LePrince, S., 2018. ECOsystem Spaceborne Thermal Radiometer Experiment on Space Station Level-1B Resampling and Geolocation Algorithm Theoretical Basis Document (ATBD) (No. JPL D95641 Version 1.0 Rev 2).

Song, L., Kustas, W.P., Liu, S., Colaizzi, P.D., Nieto, H., Xu, Z., Ma, Y., Li, M., Xu, T., Agam, N., 2016. Applications of a thermal-based two-source energy balance model

using Priestley-Taylor approach for surface temperature partitioning under advective conditions. J. Hydrol. 540, 574–587.
Stanturf, J.A., Palik, B.J., Dumroese, R.K., 2014. Contemporary forest restoration: a review emphasizing function. For. Ecol. Manag. 331, 292–323.
Stavros, E.N., Schimel, D., Pavlick, R., Serbin, S., Swann, A., Duncanson, L., Fisher, J.B., Fassnacht, F., Ustin, S., Dubayah, R., 2017. ISS observations offer insights into plant function. Nat. Ecol. Evol. 1, 1–5.
Strader, M., 2017. A Long-Term Look at the Future of Albion Hills Conservation Area. Toronto.com.
Suganuma, M.S., Durigan, G., 2015. Indicators of restoration success in riparian tropical forests using multiple reference ecosystems: indicators of riparian forests restoration success. Restor. Ecol. 23, 238–251. https://doi.org/10.1111/rec.12168.
Tobner, C.M., Paquette, A., Reich, P.B., Gravel, D., Messier, C., 2014. Advancing biodiversity–ecosystem functioning science using high-density tree-based experiments over functional diversity gradients. Oecologia 174, 609–621.
Tuff, K.T., Tuff, T., Davies, K.F., 2016. A framework for integrating thermal biology into fragmentation research. Ecol. Lett. 19, 361–374.
Ulanowicz, R.E., Hannon, B.M., 1987. Life and the production of entropy. Proc. R. Soc. Lond. B 232, 181–192. https://doi.org/10.1098/rspb.1987.0067.
Xiao, J., Fisher, J.B., Hashimoto, H., Ichii, K., Parazoo, N.C., 2021. Emerging satellite observations for diurnal cycling of ecosystem processes. Nat. Plants 1–11.
Xue, J., Anderson, M.C., Gao, F., Hain, C., Sun, L., Yang, Y., Knipper, K.R., Kustas, W.P., Torres-Rua, A., Schull, M., 2020. Sharpening ECOSTRESS and VIIRS land surface temperature using harmonized Landsat-sentinel surface reflectances. Remote Sens. Environ. 251, 112055.
Zuur, A., Ieno, E.N., Walker, N., Saveliev, A.A., Smith, G.M., 2009. Mixed Effects Models and Extensions in Ecology with R. Springer, New York, NY.